World Academy of Science, Engineering and Technology
International Journal of Electronics and Communication Engineering
Vol:15, No:6, 2021

Miniaturized Wideband Single-Feed Shorted-Edge Stacked Patch Antenna for C-Band Applications

Abdelheq Boukarkar, Omar Guermoua

***Abstract*—**In this paper, we propose a miniaturized and wideband patch antenna for C-band applications. The antenna miniaturization is obtained by loading shorting vias along one patch edge. At the same time, the wideband performance is achieved by combining two resonances using one feed line. The measured results reveal that the antenna covers the frequency band 4.32 GHz to 6.52 GHz (41%) with a peak gain and a peak efficiency of 5.5 dBi and 87%, respectively. The antenna occupies a relatively small size of only 26 x 22 x 5.6 mm^3, making it suitable for compact wireless devices requiring a stable unidirectional gain over a wide frequency range.

***Keywords*—**Miniaturized antennas, patch antennas, stable gain, wideband antennas.

I. Introduction

IN recent years, the need for designing small size radio frequency (RF) devices is increasing significantly. Indeed, modern wireless systems require antennas with lightweight, low profile, and low cost that can be integrated into the RF front end easily. Patch antennas are attractive candidates as they meet the requirements mentioned above. However, in some wireless applications, a conventional patch antenna may not be suitable due to its narrow impedance bandwidth of less than 5% in most cases. Hence, bandwidth enhancement is needed under the constraints of maintaining a compact size and a stable gain with unidirectional radiation patterns.

Several works targeting bandwidth enhancement of patch antennas have been proposed [1]-[15]. The common method of improving the working bandwidth consists of introducing slots adequately into the antenna structure [1]-[7]. By controlling the shape and the position of the slots, different resonant modes can be excited and combined accordingly to widen the working bandwidth. An illustrative example is demonstrated in [2], where a V-shaped slot is etched on the radiating triangular patch to enhance the impedance bandwidth. In this design, an additional resonant mode TM_{11} is generated by the insertion of the V-shaped slot. Another approach of bandwidth enhancement exploits the coupling between the main radiating element and some parasitic strips or patches [8]-[12]. For instance, in [8], two additional resonances are obtained by introducing multiple parasitic patches which are placed carefully near a radiating triangular element. By adopting this technique, a considerable improvement of the working bandwidth is realized (about 13.8% evaluated at 10 dB of return loss). Metamaterials can also be used to broaden the working bandwidth, as illustrated in [13]-[15]. For instance, in [13], a metamaterial-based rectangular patch antenna with wideband performance is obtained by manipulating the structure and the position of an additional metasurface. The antenna's impedance bandwidth is enhanced clearly as it reaches 36%.

In this paper, the proposed approach consists of combining two resonances from two shorted radiating patches. Shorting vias are loaded carefully along one radiating edge for antenna miniaturization. The radiating elements are fed concurrently for more antenna compactness. The operating frequencies are controlled easily by adjusting the length of the patches. The proposed antenna realizes a comparatively wide operating bandwidth of 41% on a relatively small platform of 26 x 22 x 5.6 mm^3. The antenna can be employed in c-band applications, for instance, in Worldwide Interoperability for Microwave Access (WiMAX), working around 5.8 GHz.

The paper is organized as follows. In Section II, the antenna design guidelines, including the working mechanism, are provided. In Section III, the simulated and measured results, as well as a comparison study with some recent works, are given. The conclusion of this work is drawn in Section IV.

II. Antenna Geometry and Design Guidelines

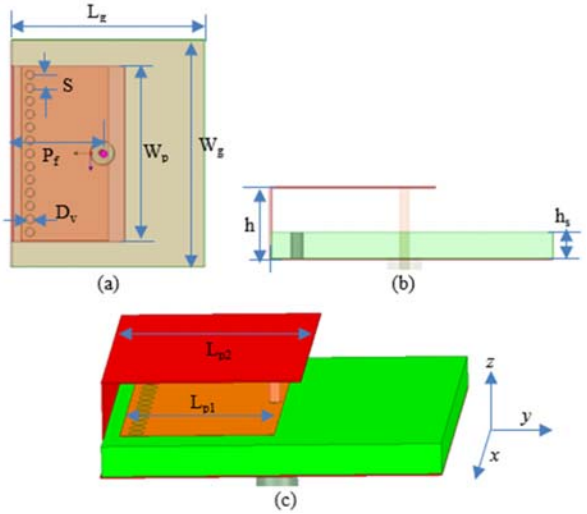

Fig. 1 Structure of the proposed antenna; (a) top view, (b) side view, (c) perspective view

The antenna's geometry is given in Fig. 1, and its dimensions are depicted in Table I. The antenna consists of two radiating

A. Boukarkar and O. Guermoua are with Ècole Supérieure Ali Chabati, Algiers, 16000, Algeria (phone: +213666570816; email: abdelheq.boukarkar@gmail.com).

patches. The first radiating patch is printed on the F4B substrate with a thickness of h_s = 2 mm, a relative permittivity of ε_r = 2.65, and a loss tangent of 0.002. Metalized vias are loaded onto one radiating edge to reduce the patch's length by approximately a half. At the same time, a sheet of copper is bent and soldered adequately to the antenna's ground plane to form the second radiating patch. The two patches are fed simultaneously using a probe feed coaxial cable. The position of the probe feed P_f controls the bandwidth impedance. The lengths of the patches L_{p1} and L_{p2} are evaluated using the following equations:

$$L_{p1} = \frac{\lambda g_1}{4} + h_s \quad (1)$$

$$\lambda g_1 \approx \frac{c}{f_1\sqrt{\varepsilon_r}} \quad (2)$$

$$L_{p2} = \frac{\lambda g_2}{4} + h \quad (3)$$

$$\lambda g_2 \approx \frac{c}{f_2\sqrt{\varepsilon_r}} \quad (4)$$

where λ_{g1} and λ_{g2} are the guided wavelengths corresponding to the operating frequencies f_1 and f_2, respectively. The antenna resonances are combined adequately to broaden the impedance bandwidth. The antenna working frequencies are chosen arbitrarily to cover some C-band applications. Indeed, one can easily select the working bandwidth by adjusting the length of the two patches L_{p1} and L_{p2}.

TABLE I
ANTENNA DIMENSIONS

Parameter	W_g	L_g	L_{p1}	L_{p2}	h	h_s	W_p	P_f	D_v	S
Value (mm)	26	22	10	12.8	5.6	2	20	10.5	1	1.5

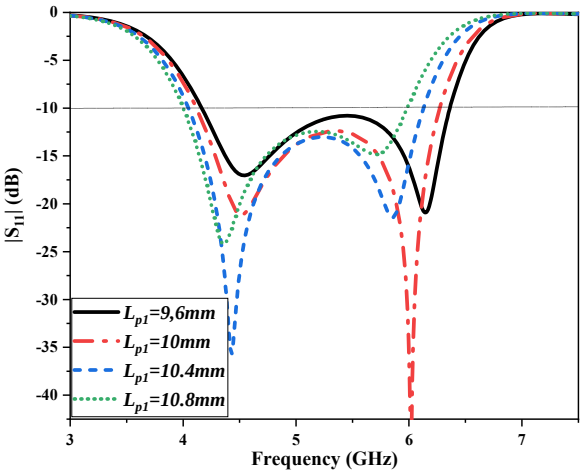

Fig. 2 The simulated reflection coefficient $|S_{11}|$ when the length of the patch L_{p1} is tuned

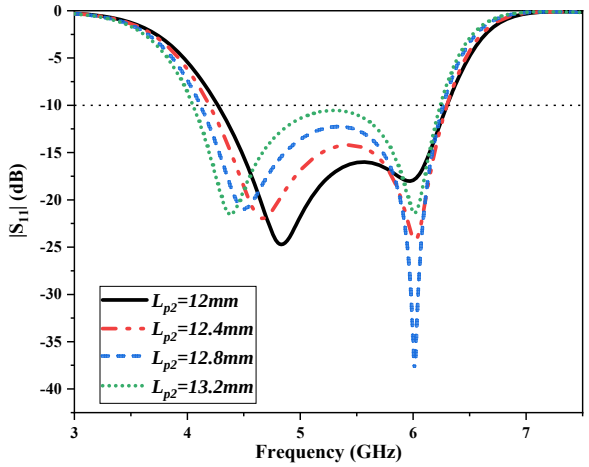

Fig. 3 The simulated reflection coefficient $|S_{11}|$ when the length of the patch L_{p2} is tuned

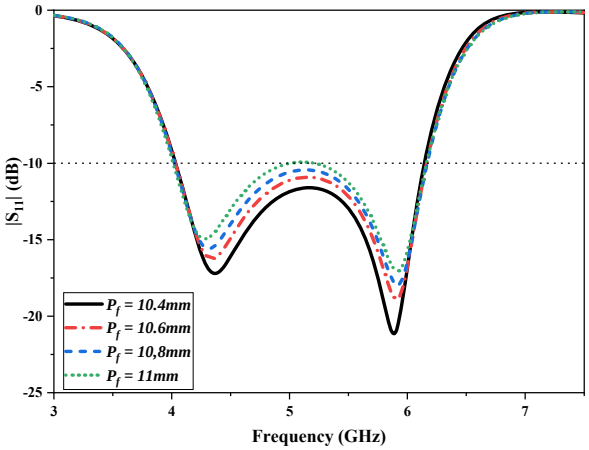

Fig. 4 The simulated reflection coefficient $|S_{11}|$when the position of the feed point P_f is tuned

To understand more the working mechanism and the design guidelines, three parametric studies are performed using High-Frequency Structure Simulator (HFSS) software. The first parametric study investigates the effects of tuning the patch's length L_{p1} on the resonant frequencies. We note that the lower operating frequency remains stable during the tuning of L_{p1}, as shown in Fig. 2. Similarly, we have concluded from the second parametric study that the lower operating frequency can be controlled by adjusting the length L_{p2} without affecting much the upper resonance. The corresponding reflection coefficient $|S_{11}|$ is shown in Fig. 3. The last parametric study deals with the position of the feed line P_f. Indeed, the antenna impedance matching is ensured easily by selecting an adequate feed position P_f as demonstrated in Fig. 4. The current distribution, at the lower and the upper resonant frequencies, is given in Fig. 5. We note that each patch can be excited separately. To validate the proposed approach, an antenna prototype is fabricated and tested. The next section is devoted to the simulation and measurement results.

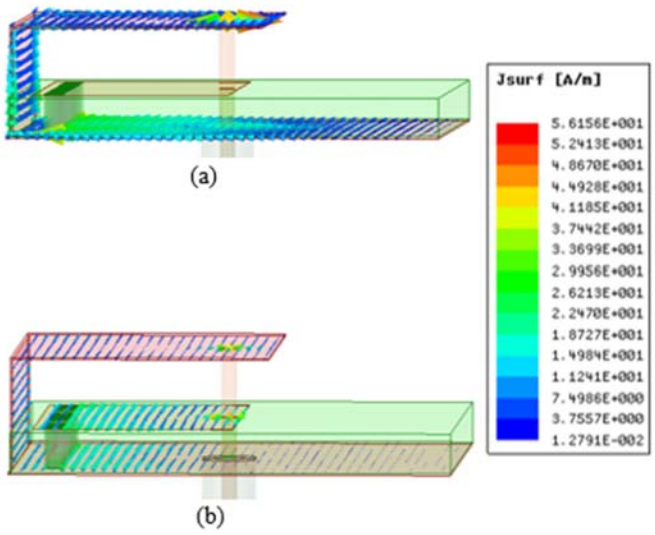

Fig. 5 The current distribution at the resonant frequencies; (a) f_1 = 4.2 GHz, (b) f_2 = 6.2 GHz

III. Simulated and Measured Results

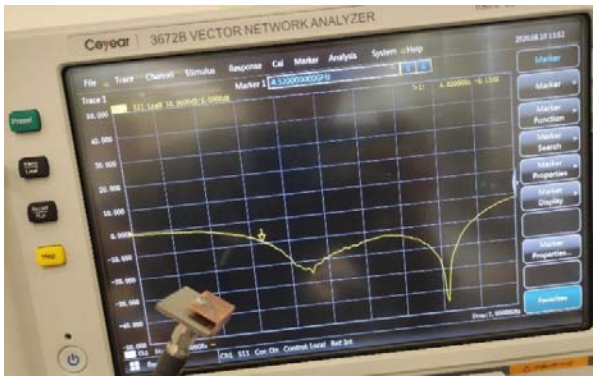

Fig. 6 Photograph of the antenna with the $|S_{11}|$ measurement setup

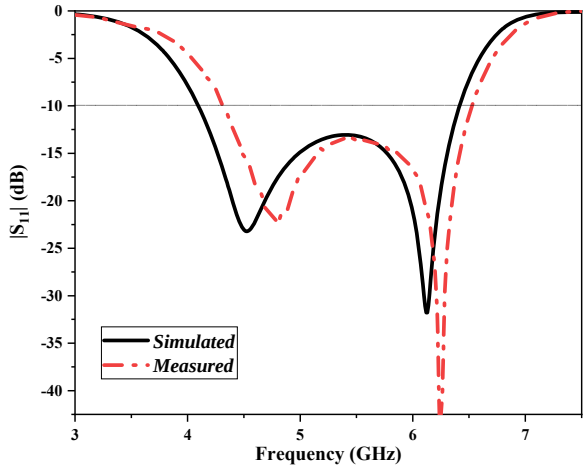

Fig. 7 The simulated and measured reflection coefficient $|S_{11}|$

The photograph of the fabricated antenna with the $|S_{11}|$ measurement setup is shown in Fig. 6. The second radiating patched formed by the copper sheet is soldered carefully to the antenna's ground plane. The antenna reflection coefficient is measured using a 3672B vector network analyzer. The simulated and measured $|S_{11}|$ is shown in Fig. 7.

The measured results reveal that the antenna covers the operating band 4.32 GHz to 6.65 GHz with a good impedance matching. The small discrepancies between the simulated and measured results are attributed mainly to the measurement setup and fabrication tolerances. The antenna radiation patterns are obtained in SATIMO anechoic chamber. The radiation patterns measurement setup is shown in Fig. 8.

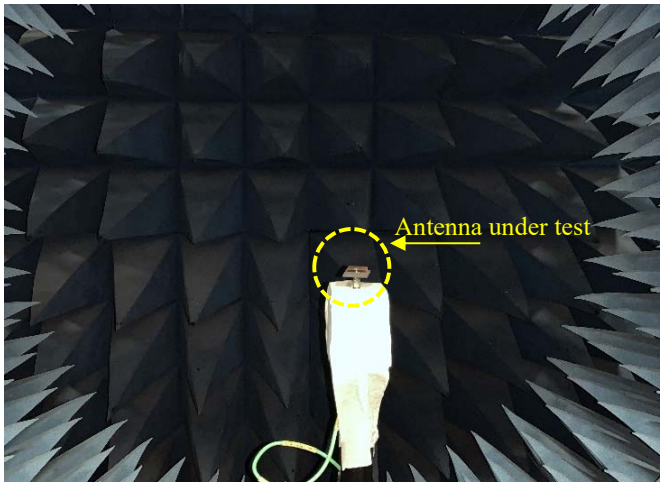

Fig. 8 The radiation pattern measurement setup

TABLE II
Comparison Study

Reference	[7]	[9]	[15]	Proposed
Size (λ_0)	0.52 x 0.35 x 0.06	1.09 x 1.09 x 0.03	0.36 x 0.36 x 0.04	0.37 x 0.31 x 0.08
Frequencies (GHz)	1.62–2.78	2.19–2.68	5.31–5.92	4.32–6.52
Bandwidth (%)	52.7	20.1	10.86	41%
Average gain (dBi)	6	9.5	4.17	5
Average efficiency (%)	N.M*	88	72	85
Approach	Etching slots	Parasitic patches	Metamaterials loading	Stacked shorted patches

We note that λ_0 is the free-space wavelength evaluated at the lower limit of the working bandwidth. * N.M: Not Mentioned.

To demonstrate the stability of the patterns, three frequency samples are selected. The frequency points correspond to the lower, the middle, and the upper limit of the operating bandwidth. The simulated and measured patterns at f_L = 4.32 GHz, f_m = 5.42 GHz, and f_u = 6.52 GHz are compared in Fig. 9. We note that, in all the cases, the simulated and measured results agree well. The measured gains and efficiencies vary from 4.3 dBi to 5.5 dBi and 82% to 87%, respectively. To highlight the contributions made in this paper, a comparison study with some recently published papers is displayed in Table II. The antennas' sizes, operating frequencies, bandwidths, average gains, efficiencies, and the used approaches are provided. The design in [7] realizes a comparatively wide bandwidth of 52.7% with an average gain of 6 dBi. In comparison, the proposed design has a slightly smaller size. The

antenna presented in [9] occupies a larger area with comparatively higher gain and 20.1% of impedance bandwidth. In [15], the antenna has a compact size; however, its impedance bandwidth is relatively low. One can note the trade-off between antenna profile and the working bandwidth. The larger the profile is, the wider the impedance bandwidth.

The proposed antenna exhibits acceptable performance in terms of overall size, operating bandwidth, and average gain. In current wireless systems, compact RF components are highly recommended. As the proposed design is small, it can be used to form an antenna array.

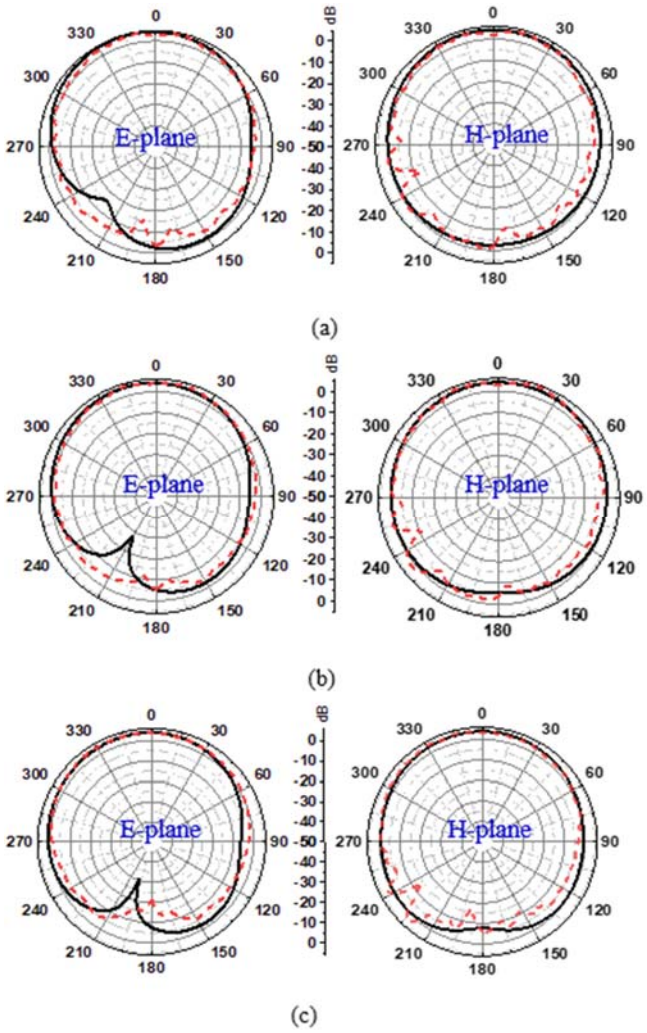

Fig. 9 The simulated and measured radiation pattern (sold line: simulated, dashed line: measured); (a) f_L = 4.32 GHz, (b) f_m = 5.42 GHz, (c) f_u = 6.52 GHz

IV. Conclusion

In this paper, a simple design of a miniaturized patch antenna with wideband performance is achieved. The two operating frequencies are combined and controlled easily by adjusting the corresponding patch lengths L_{p1} and L_{p2}. The antenna exhibits comparatively acceptable performances in terms of operating bandwidth, gain, and efficiency with a miniaturized size of only 26 x 22 x 5.6 mm^3. As a suggestion for future work, the proposed design may be used as an antenna element of a miniaturized phased array antenna covering some C-band applications.

References

[1] M. Min and L. Guo, "Design of a Wideband Single-Layer Reflectarray Antenna Using Slotted Rectangular Patch with Concave Arms," IEEE Access, vol. 7, pp. 176197-176203, 2019.

[2] H. Wong, K. K. So and X. Gao, "Bandwidth Enhancement of a Monopolar Patch Antenna With V-Shaped Slot for Car-to-Car and WLAN Communications," IEEE Transactions on Vehicular Technology, vol. 65, no. 3, pp. 1130-1136, March 2016.

[3] N. Liu, L. Zhu and W. Choi, "A Low-Profile Wide-Bandwidth Planar Inverted-F Antenna Under Dual Resonances: Principle and Design Approach," IEEE Transactions on Antennas and Propagation, vol. 65, no. 10, pp. 5019-5025, Oct. 2017.

[4] A. Bekasiewicz and S. Koziel, "Cost-Efficient Design Optimization of Compact Patch Antennas with Improved Bandwidth," IEEE Antennas and Wireless Propagation Letters, vol. 15, pp. 270-273, 2016.

[5] T. F. A. Nayna, F. Ahmed and E. Haque, "Bandwidth enhancement of a rectangular patch antenna in X band by introducing diamond shaped slot and ring in patch and defected ground structure," 2017 International Conference on Wireless Communications, Signal Processing and Networking (WiSPNET), Chennai, 2017, pp. 2512-2516.

[6] N. Liu, L. Zhu and W. Choi, "A Differential-Fed Microstrip Patch Antenna with Bandwidth Enhancement Under Operation of TM10 and TM30 Modes," IEEE Transactions on Antennas and Propagation, vol. 65, no. 4, pp. 1607-1614, April 2017.

[7] W. An, X. Wang, H. Fu, J. Ma, X. Huang and B. Feng, "Low-Profile Wideband Slot-Loaded Patch Antenna with Multiresonant Modes," in IEEE Antennas and Wireless Propagation Letters, vol. 17, no. 7, pp. 1309-1313, July 2018.

[8] K. D. Xu, H. Xu, Y. Liu, J. Li and Q. H. Liu, "Microstrip Patch Antennas with Multiple Parasitic Patches and Shorting Vias for Bandwidth Enhancement," IEEE Access, vol. 6, pp. 11624-11633, 2018.

[9] D. Yang, H. Zhai, C. Guo and H. Li, "A Compact Single-Layer Wideband Microstrip Antenna with Filtering Performance," IEEE Antennas and Wireless Propagation Letters, vol. 19, no. 5, pp. 801-805, May 2020.

[10] Z. Liang, J. Liu, Y. Zhang and Y. Long, "A Novel Microstrip Quasi Yagi Array Antenna with Annular Sector Directors," IEEE Transactions on Antennas and Propagation, vol. 63, no. 10, pp. 4524-4529, Oct. 2015.

[11] J. Wu, Y. Yin, Z. Wang and R. Lian, "Broadband Circularly Polarized Patch Antenna with Parasitic Strips," IEEE Antennas and Wireless Propagation Letters, vol. 14, pp. 559-562, 2015.

[12] J. Zhang, L. Zhu, Q. Wu, N. Liu and W. Wu, "A Compact Microstrip-Fed Patch Antenna with Enhanced Bandwidth and Harmonic Suppression," IEEE Transactions on Antennas and Propagation, vol. 64, no. 12, pp. 5030-5037, Dec. 2016.

[13] N. Nasimuddin, Z. N. Chen and X. Qing, "Bandwidth Enhancement of a Single-Feed Circularly Polarized Antenna Using a Metasurface: Metamaterial-based wideband CP rectangular microstrip antenna.," in IEEE Antennas and Propagation Magazine, vol. 58, no. 2, pp. 39-46, April 2016.

[14] S. Ahdi Rezaeieh, M. A. Antoniades and A. M. Abbosh, "Gain Enhancement of Wideband Metamaterial-Loaded Loop Antenna with Tightly Coupled Arc-Shaped Directors," IEEE Transactions on Antennas and Propagation, vol. 65, no. 4, pp. 2090-2095, April 2017.

[15] M. Ameen and R. K. Chaudhary, "Metamaterial-based circularly polarised antenna employing ENG-TL with enhanced bandwidth for WLAN applications," Electronics Letters, vol. 54, no. 20, pp. 1152-1154, 2018.